# NASA Scatterometer Observes the Extratropical Transition of Pacific Typhoons

W. Timothy Liu, Wenqing Tang, and R. Scott Dunbar

Jet Propulsion Laboratory 300-323

California Institute of Technology

Pasadena, CA 91109

Tel: 818-354-2394

Fax: 818-393-6720

Email:liu@pacific.jpl .nasa.gov

During its first ten days of the ocean observing mode, starting 15 September 1996, the National Aeronautics and Space Administration (NASA) Scatterometer (NSCAT) monitored the evolution of the twin typhoons Violet and Tom. They moved north from the western tropical Pacific, acquiring the features of mid-latitude storms, with developing frontal structures, increasing asymmetry, and introduction of dry air into the core of the typhoons. While Violet hit Japan, causing destruction and death (Fig. 1), Tom merged with a mid-latitude trough and evolved into a large extratropical storm with gale-force winds (Fig. 2).

We understand relatively little of the extratropical transition of tropical cyclones because of the complex thermodynamics involved [e.g., Sinclair, 1993]. Since the transition usually occurs over the ocean, there has been very little measurements of it. Yet the mid-latitude storms resulting from tropical cyclones usually have strong winds and heavy precipitation. The transition is a fascinating science problem, but it also has important economic consequences. The transition occurs over the busiest trams-ocean shipping lane, and when the resulting storms hit land, they usuall y cause devastation to populated areas.

NSCAT was successfully launched into a near-polar, sun-synchronous orbit on the Japanese Advanced Earth Observing Satellite (ADEOS) in August 1996 from Tanegashima Space Center in Japan. The six antennas of NSCAT send microwave pulses at a frequency of 14 GHz to the Earth's surface and measure the backscatter. The antennas scan two 600-km bands of the ocean which are separated by a 330-km data gap. From NSCAT observations, surface wind vectors can be derived at 25-km spatial resolution, covering 7'7% of the ice-free ocean in one day and 97% of the ocean in two days, under both clear and cloudy conditions. Together with the precipitable water (vertically integrated water vapor) derived from the Special Sensor Microwave / Imager (SSM/I) on the operational spacecraft of the Defense Meteorological Space Program (DMSP), the wind observations provide a good opportunity to monitor and understand the evolution of Violet and Tom. The precipitable water from SSM/I has been evaluated by Liu et al. [1992] and others. The detailed structure of the wind-field in Fig. 1 illustrates the high spatial resolution of NSCAT. The abrupt change in wind direction northeast of the core is likely to be have been caused by the development of frontal structure. The overlay of wind on precipitable water dramatically visualizes not only the structure of this evolving system, but also the relation between the dynamics and the hydrologic balance in the mesoscale.

The best-track analyses from typhoon centers and the surface weather maps put out by the National Weather Service (NWS) indicate both Typhoons Tom and Violet were both born approximate] y on September 11 in the western tropical Pacific at 8°N, with Violet at 130°E and Tom at 150°E, before NSCAT data were available. In the observations for September 16, the two spaceborne sensors clearly identifies Typhoon Tom (at the lower left corner of Fig. 2a), with high cyclonic surface wind. A family of mid-latitude cyclones is revealed at 35”N by NSCAT winds. There are two centers of wind speed minima and cyclonic relative vorticity, at 152°E and 158°E. The former is an old occluded system that evolved from a cyclone on the previous day, while the latter is an incipient system with clear warm and cold fronts. On the 17th, NSCAT observed the development of a third cyclone centered at 167°E and the occlusion of the cyclone at 158°E. For these three days, September 15-17, the surface weather maps from NWS and the numerical weather prediction (NWS) data of the National Center for Environmental Prediction (NCEP), with low spatial resolutions, allow only the identification of a single low pressure center at 35”N, moving from 148°E on the 15th, to 156°E on the 16th, and on to 166°E on the 17th. The advantage of NSCAT observation is clearly evident in comparison. While there were no NSCAT data during an ADEOS check-out period between the 17th and 18th, the surface weather maps indicate that the low-level trough remains at around 35”N, with its center moving east to near 180°E. On the 19th, Typhoon Tom moved in and merged with the extratropical system.

During the three days of active cyclogenesis at 35°N, Typhoon Tom moved very slowly, with slight development of a frontal structure in the east. In Fig. 2a, Tom can be distinguished from the extratropical cyclones by the high water vapor (and diabatic heating generated by latent heat release) concentrated in the core. There is much less water vapor in the extratropical cyclones, with a slightl y high value in the warm sector between the fronts, but not at the core. Tom speeded up on the 18th and moved toward the northeast, keeping a high amount of water vapor at the core. On September 19, Typhoon Tom moved into the trough at 35°N. It lost much of the water vapor during this process, but still kept unusually high water vapor at the frontal location, compared with previous extratropical cyclones (Fig. 2b). This high water vapor was clearly observed by SSM/I in the next few days as the system resulting from Tom moved east. Both NCEP and NSCAT data indicate strong winds above 25 m/s for this extratropical system that resulted from Tom, but the maximum winds from NSCAT are located to the west, while the maximum winds from NCEP are located to the east, of the cyclone.

The atmosphere and its clouds are much more transparent to radiation at microwave than at visible or infrared frequencies, The combination of an active (NSCAT) and a passive (SSM/I) microwave sensor provides good observations for weather systems accompanied by cloud cover. In this case, the two sensors revealed the evolution of tropical cyclones from a warm core system into more baroclinic mid-latitude storms with unusuall y strong wind and high precipitation. However, even microwave sensors are contaminated by rain and the accuracy of scatterometer winds above 25 m/s has not been sufficiently validated. The NSCAT data used in this study are interim products retrieved using a prelaunch model function developed by Wentz et al. [1994]. Vigorous validation efforts are underway and an improved model function is being developed. McMurdie et al. [1987] used a combination of microwave scatterometer and radiometer data to study mid-latitude cyclones. Hsu and Liu [1996] used scatterometer winds to derive their surface pressure field and to provide an improved description of the location and intensity of tropical cyclones. Hsu et al. [1997] demonstrated that scatterometer winds can be used to improve significantly the surface divergence, vertical velocity profile, and, therefore, the heat and hydrologic budgets of convective systems, These methodologies can be used to further our understanding of the thermodynamics of the extratropical transition of tropical cyclones.


## Acknowledgments

This study was performed at the Jet Propulsion Laboratory, California Institute of Technology, under contract with the National Aeronautics and Space Adminstration (NASA). It was jointly supported the NSCAT Project, the Earth Observing System (EOS) Interdisciplinary Science Program, and the Physical Oceanography Branch of the Mission to Planet Earth. Some of the SSMI data were obtained from the EOS Distributed Active Archive Center at Marshall Space Flight Center; some were also kindly provided by Frank Wentz. We are grateful to Johnny C.L. Chan for information on past studies of typhoon transition.


## References


Hsu, C.S. and W.T. Liu, 1996: Wind and pressure fields near Tropical Cyclone Oliver derived from scatterometer observations. *J. Geophys. Res.*, ***101***, 17,021-17,027.

Hsu, C. S., W.T. Liu, and M.G. Wurtele, 1997: Impact of scatterometer winds on hydrologic forcing and convective heating through surface divergence. *Mon. Wea. Rev.*, 125, No. 7, in press.

Liu, W.T., W. Tang and F.J. Wentz, 1992: Precipitable water and surface humidity over global oceans from Special Sensor Microwave Imager and European Center for Medium Range Weather forecasts. *J. Geophys. Res.*, 97, 2251-2264.

McMurdie, L., G. Levy, and K.B. Katsaros, 1987: On the relationship between scatterometer-derived convergence and atmospheric moisture. *Mon. Wea. Rev.*, *115*, 1281-1294.

Tang, W., and W.T. Liu, 1996: *Objective Interpolation of Scatterometer Winds.* JPL Publication %-19, Jet Propulsion Laboratory, Pasadena, 20 pp.

Sinclair, M. R., 1993: Synoptic-scale diagnosis of the extratropical transition of a southwest Pacific tropical cyclone, Mon. *Wea. Rev., 121, 941-960.*

Wentz, F. J., S. Peteherych, and L.A. Thomas, 1984: A model function for ocean radar cross sections at 14.6 GHz. *J. Geophys. Res., 89, 3689-3704.*

## List of Figures

Fig. 1 Typhoon Violet is revealed by the wind vectors (dark arrows) and the integrated water vapor (color image) on 21 September 1996, just before it hits Japan, causing damage and death. The wind and water vapor are derived from the observations by NSCAT on ADEOS and SSM/I on DMSP F-13, along their respective ascending orbits, which are roughly five hours apart.

Fig. 2 Evolution of Typhoon Tom revealed by surface wind (dark arrows) and integrated water vapor (color image) fields at O UTC on September 16 (a) and September 19 (b), derived from NSCAT and SSM/I observations by using an objective interpolation scheme described by Tang and Liu [1996], but without using any other data for initialization.

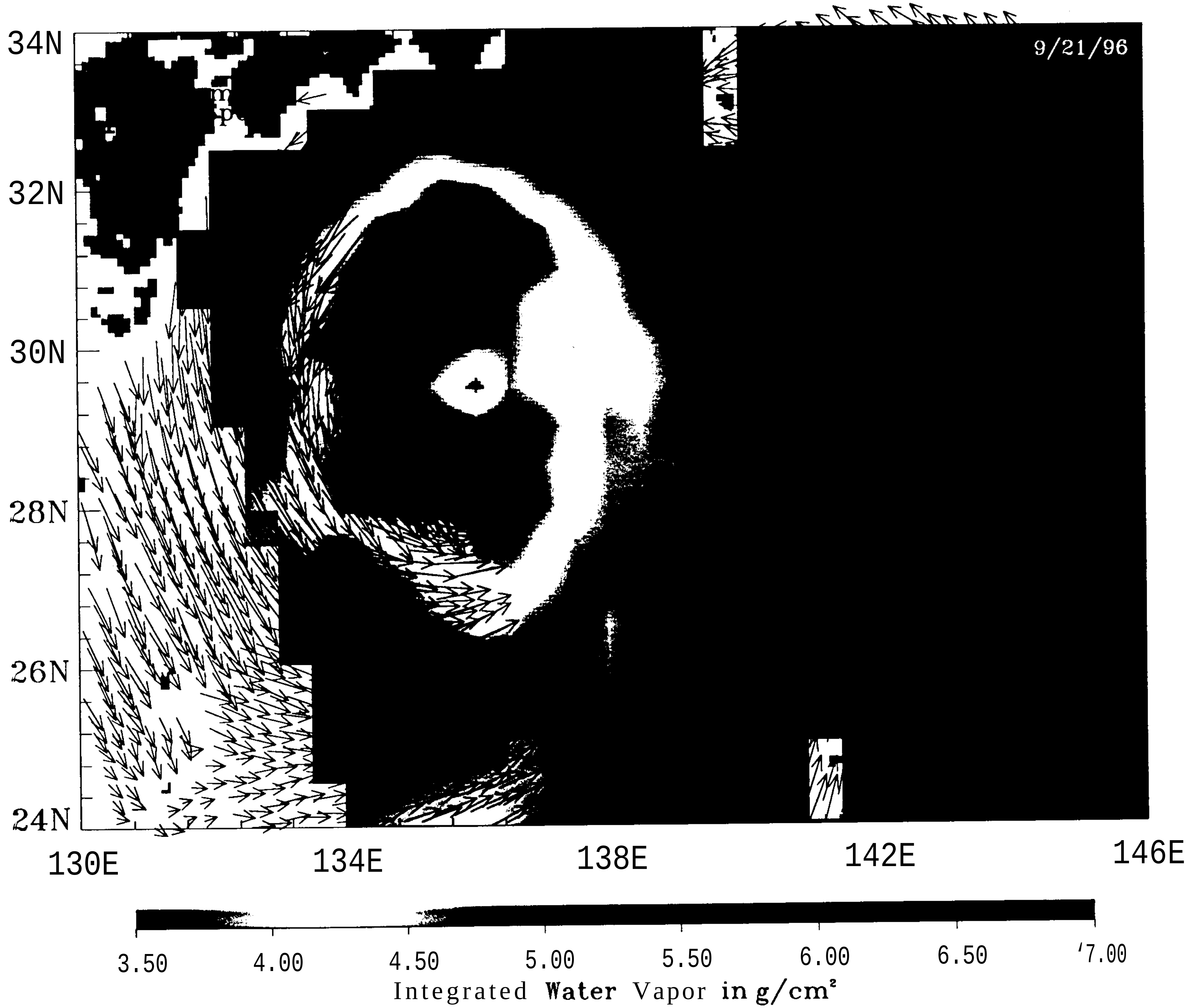
9/21/96
34N
32N
30N
28N
26N
24N
130E
134E
138E
142E
146E
3.50
4.00
4.50
5.00
5.50
6.00
6.50
7.00
Integrated Water Vapor in g/cm²

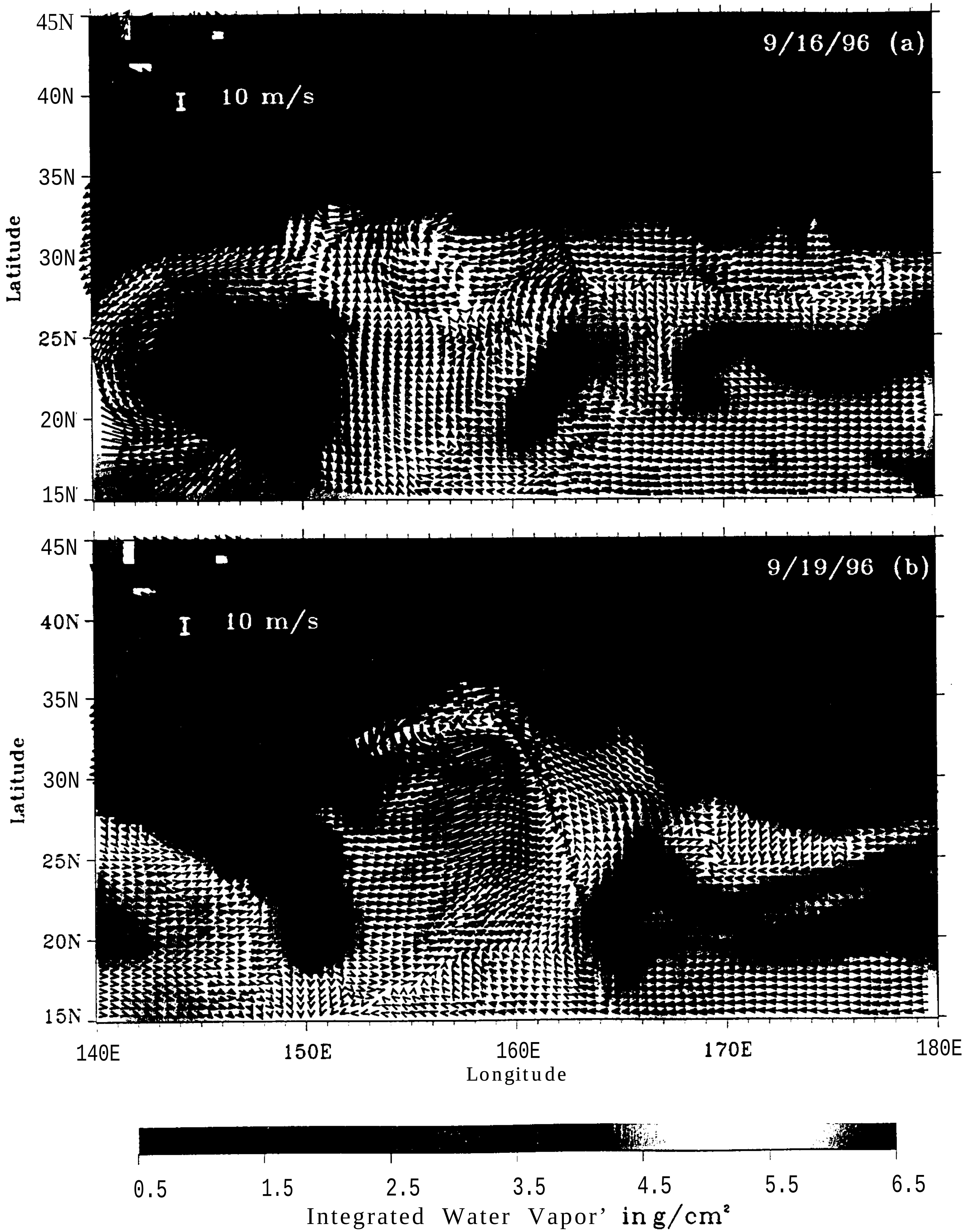

9/16/96 (a)
10 m/s
45N
40N
35N
30N
25N
20N
15N
Latitude
9/19/96 (b)
10 m/s
140E
150E
160E
170E
180E
Longitude
0.5
1.5
2.5
3.5
4.5
5.5
6.5
Integrated Water Vapor' in g/cm²